International Journal of Solids and Structures 51 (2014) 1123–1131

Contents lists available at ScienceDirect

International Journal of Solids and Structures

journal homepage: www.elsevier.com/locate/ijsolstr

Cohesive zone model for high-cycle fatigue of adhesively bonded joints under mode I loading

M.F.S.F. de Moura [a,*], J.P.M. Gonçalves [b]

[a] Faculdade de Engenharia da Universidade do Porto, Departamento de Engenharia Mecânica, Rua Dr. Roberto Frias, 4200-465 Porto, Portugal
[b] IBM T.J. Watson Research Center, 1101 Kitchawan Road, Yorktown Heights, NY 10598, USA

ARTICLE INFO

Article history:
Received 26 July 2013
Received in revised form 5 November 2013
Available online 12 December 2013

Keywords:
Cohesive zone model
High-cycle fatigue
Adhesively bonded joints
Mode I loading

ABSTRACT

A cohesive zone model adequate for simulating the behaviour of adhesively bonded joints subjected to high-cycle fatigue and pure mode I loading is presented. The bilinear cohesive zone law with linear softening relationship was considered. The main advantage of the proposed formulation is the use of a unique damage parameter accounting for cumulative damage resulting from static and fatigue loading. The method was implemented in a user subroutine of the commercial finite element software Abaqus®. Two-dimensional numerical simulations of the double cantilever beam test using different representative combinations of the modified Paris law coefficients were performed. It was verified that the results of the model simulate with excellent agreement the several Paris laws used as input, thus demonstrating the good performance of the method as a predictive tool.

1. Introduction

Adhesively bonded joints are nowadays widely used in several industries such as automotive and aerospace. They have been increasingly adopted in structural applications due to their many advantages over classical mechanically fastened joints. Some of those advantages are lower weight, more uniform distribution of load, and better fatigue performance.

The increase use of adhesively bonded joints in structural applications has been accompanied by an increase interest in the development of models that can predict the behaviour of those joints under different types of loading. A very attractive way of modelling these joints is to use the finite element method in combination with the cohesive zone model (CZM). The proponents of the CZM were Dugdale (1960) and Barenblatt (1962) and its combination with the finite element method was introduced by Hillerborg et al. (1976). Since those ideas were proposed, a significant number of studies have been published where the CZM and interface elements have been used to study the initiation and propagation of damage in several types of structures and materials subjected to monotonic loads. Examples are studies of delamination in laminated composite materials (Schellekens and de Borst, 1993; Reddy et al., 1997; Mi et al., 1999; de Moura et al. 2000) and studies of crack initiation and growth in adhesively bonded joints (Yang et al., 1999; Sørensen, 2002; Gonçalves et al., 2003; de Moura et al., 2012). Contrary to fracture mechanics based methods, the CZM provides the capability to simulate the initiation and propagation of damage without requiring the definition of an initial crack. This type of model is based on a relationship between stresses and relative displacements at points where damage can occur. Usually, the CZM is embedded in interface finite elements and these are used to model the regions of the structure where initiation and propagation of damage is likely. In bonded joints, the interface finite elements are usually used to model the thin adhesive layer where adhesive or cohesive failure occurs (de Moura et al., 2012).

Fatigue is an important type of loading for many structures that contain adhesively bonded joints. Therefore, it is important to accurately predict the fatigue strength of these joints and several methods have been developed for that purpose (Wahab, 2012). Recently, the framework for modelling adhesively bonded joints described above has been adapted in several studies to the modelling of fatigue initiation and propagation in bonded joints and in laminated composite materials. In general, those studies combine the CZM and interface elements with a fatigue damage evolution law to simulate fatigue degradation. In some of those studies (see for example Nguyen et al., 2001; Roe and Siegmund, 2003) the fatigue damage accumulation is computed cycle-by-cycle. This strategy has a very high computational cost and it is impractical for the study of high-cycle fatigue. To overcome this limitation, a strategy where it is assumed that several fatigue cycles occur between each update of the accumulated damage has been proposed and it is used in all the studies described below. Robinson et al. (2005) modified an interface finite element previously developed, and previously applied to predict delamination growth due to monotonic loading in laminated composites, to incorporate the effects

* Corresponding author. Tel.: +351 225081727.
E-mail address: mfmoura@fe.up.pt (M.F.S.F. de Moura).

0020-7683/$ - see front matter © 2013 Elsevier Ltd. All rights reserved.
http://dx.doi.org/10.1016/j.ijsolstr.2013.12.009

of cyclic loading. The constitutive law implemented in the original interface element was extended by incorporating a modified version of a continuum fatigue damage model. Numerical results showed that the model replicates the behaviour of the modified Paris law observed in experimental testing. Muñoz et al. (2006) tested the computational robustness of the formulation described in Robinson et al. (2005) with respect to the number of cycles per increment and the element size. Their numerical results showed some limitations in the values that those parameters can take and, in particular, they showed that large interface elements can cause oscillations in the crack growth rate. Muñoz et al. (2006) also extended the formulation of Robinson et al. (2005) to include cyclic loads where the minimum value is non-zero. Turon et al. (2007) developed a CZM for modelling delamination in laminated composite materials subjected to high-cycle fatigue loading. The CZM uses a single damage variable and defines its evolution in terms of the crack growth rate. The damage state depends on the number of cycles but also takes into account the loading conditions. The model was tested for modes I, II and mixed-mode I/II loading conditions and the results showed a higher level of accuracy for mode I compared with the other modes of loading. Pirondi and Moroni (2010) introduced a procedure to predict fatigue crack growth in bonded joints that also uses a CZM with a single damage variable as presented in Turon et al. (2007). Their work includes an automated procedure to compute the applied strain energy release rate, which is not part of the model in Turon et al. (2007), and was developed for loading modes I and II. In Moroni and Pirondi (2011), the same authors extended their model to mixed mode I/II loading. In both studies, the results from the models were compared with experimental results from the literature and good agreements were obtained. Harper and Hallett (2010) developed a CZM based on a detailed study of the numerical cohesive zone and its use in the computation of the strain energy release rate. Their model was implemented in three-dimensional interface elements within the explicit finite element software LS-Dyna. They applied it to fatigue fracture toughness tests of composite materials and studied mode I, mode II, and mixed-mode I/II loading. Their numerical results showed good agreement when compared with experimental results from the literature and with theoretical solutions. May and Hallett (2010) introduced a phenomenological damage variable for fatigue damage initiation into the model previously developed in Harper and Hallett (2010). Their objective was to better model fatigue initiation in the region where the modified Paris law is invalid. Their conclusion was that their model showed potential to model fatigue initiation for cases in which damage would not occur in models based on the modified Paris law. However, they identified some limitations in their new model which was not able to provide accurate predictions in some of the tests conducted. Kawashita and Hallett (2012) proposed a crack tip tracking algorithm which is used in conjunction with a CZM implemented in three-dimensional interface elements and implemented as a user-defined subroutine in LS-Dyna. Their formulation is completely independent of the cohesive zone length and it is relatively insensitive to mesh size. They applied their method to the study of delamination propagation in composite laminates under cyclic loading. The predicted delamination rates were found to be weakly dependent on mesh size. Khoramishad et al. (2010a) used a CZM integrated with a strain-based fatigue damage model to simulate fatigue damage in adhesively bonded joints. The numerical fatigue model was calibrated against experimental results obtained for single lap joints and that same model was then used to accurately predict the fatigue behaviour of laminated doublers in bending. This model was later extended by the same authors (Katnam et al., 2010; Khoramishad et al., 2010b) to take into account the effect of load ratio on the fatigue behaviour of adhesively bonded joints.

The objective of this work is to develop and numerically validate a cohesive zone model adequate to simulate high-cycle fatigue behaviour of adhesively bonded joints under pure mode I. The method is implemented in the finite element software Abaqus® by means of a user subroutine. The proposed methodology is based on the modified Paris law, which establishes a relation between crack growth rate and energy release rate. Material stiffness deterioration as a function of the number of cycles is simulated by means of a damage parameter that includes static and fatigue degradation. A data reduction scheme based on the crack equivalent concept is also proposed in order to simplify the process of monitoring the energy release rate in the course of the DCB fatigue test. Two-dimensional numerical simulations were performed in order to analyse the influence of the Paris law coefficients on the fatigue behaviour and it was verified that the model is able to properly capture that influence.

2. Cohesive zone model

2.1. Monotonic loading

Cohesive zone models have been used with success in the simulation of damage initiation and propagation at interfaces (Mi et al., 1999; Yang et al., 1999). The basis of a CZM is a constitutive relationship between tractions (σ) and relative displacements (w). The relative displacements at interfaces are obtained from the displacements of the homologous points belonging to both sides of the interface (Gonçalves et al., 2000). The most used CZM is the bilinear (Fig. 1), which includes a linear softening relationship when the local strength (σ_u) is attained. The softening region aims to reproduce several damaging phenomena at the crack tip in a non-negligible fracture process zone, thus falling under the domain of non-linear fracture mechanics. The area circumscribed by the cohesive law represents the critical strain energy release rate G_{Ic}. Thus, from Fig. 1 the following relationship can be written

$$G_{Ic} = \frac{\sigma_u w_u}{2} \tag{1}$$

where σ_u is the local strength and w_u the ultimate relative displacement leading to complete failure at the integration point. This means that G_{Ic} and σ_u are material parameters that should be known a priori to define the cohesive law. The bilinear CZM is characterised by two different relations. Before damage starts to grow,

$$\sigma = kw \tag{2}$$

being k the interfacial stiffness. After damage onset ($w > w_o$ in Fig. 1), the simulation of progressive damage in the softening region of the CZM is achieved by

$$\sigma = (1 - e_s)\, kw \tag{3}$$

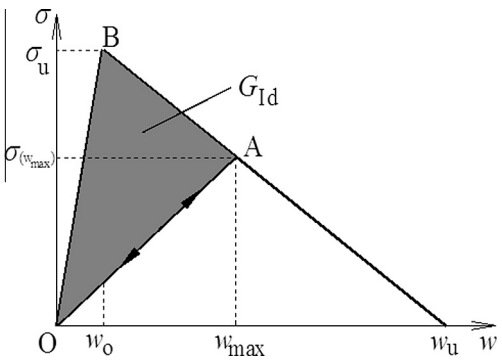

Fig. 1. Schematic representation of the cohesive law.

being e_s the damage parameter ranging between zero (undamaged case, i.e. $w = w_o$) and unity (complete failure, i.e. $w = w_u$), and given by

$$e_s = \frac{w_u(w_{max} - w_o)}{w_{max}(w_u - w_o)} \tag{4}$$

where w_o is the relative displacement corresponding to damage onset and w_{max} the maximum relative displacement reached during the loading history. For a given w inferior to w_{max} occurring during the loading history, the $\sigma = f(w)$ relationship is dictated by the line OA (Fig. 1) to avoid a healing phenomenon. Further details of the CZM can be found in references (de Moura et al., 2000; Gonçalves et al., 2000).

2.2. Fatigue loading

2.2.1. Global damage parameter

Under fatigue loading the formulation of the CZM must take into account stiffness degradation as a function of the number of cycles. In high-cycle fatigue problems the simulation of each cycle would be extremely time demanding. Consequently, loading envelopes (Fig. 2) can be used if an adequate material softening law as a function of number of cycles is considered. In order to have a general formulation accounting for monotonic (static or quasi-static) and fatigue degradation, the fatigue damage parameter e_f should be added to e_s thus defining the cumulative global damage

$$e = e_s + e_f \tag{5}$$

The global damage e must satisfy the condition $0 \leqslant e \leqslant 1$. One of the advantages of the proposed method is the use of a unique damage parameter including the global damage. This can be done using Eq. (4) and determining an equivalent w_{max} as a function of the global damage parameter e

$$w_{max} = \frac{w_u w_o}{(w_u - e(w_u - w_o))} \tag{6}$$

This equivalent w_{max} incorporates the cumulative effects of the static (e_s) and fatigue (e_f) damage on the material stiffness at a given integration point (IP). Consequently, the global damage influencing the material stiffness at a given increment and IP is embodied in the w_{max} variable, which becomes the unique damaging variable that must be continuously recorded during the incremental numeric procedure. Additionally, it is implicitly assumed that damage, independently of its origin, follows the same softening relationship (Eq. (4) where e_s is replaced by e).

2.2.2. Fatigue damage parameter

The evolution of the damage parameter e_f as a function of the number of cycles, in a given IP k belonging to the fracture process zone (FPZ), can be written as

$$\frac{de_f}{dN} = \frac{de_f}{dA_{p(k)}} \frac{dA_{p(k)}}{dN} \tag{7}$$

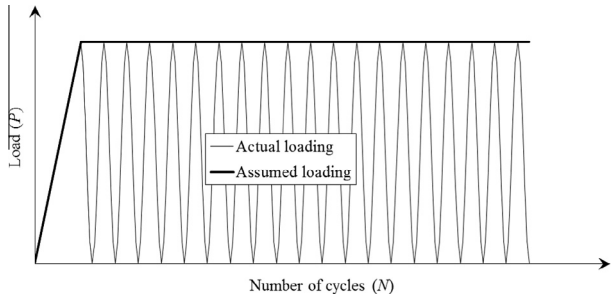

Fig. 2. Typical loading envelope considered in high-cycle fatigue model.

being $A_{p(k)}$ the local damaged area, i.e. relative to a given IP k, and N the number of cycles. The differentiation in the first term of Eq. (7) can be rewritten as

$$\frac{de_f}{dA_{p(k)}} = \frac{de_f}{dw_{max}} \frac{dw_{max}}{dA_{p(k)}} \tag{8}$$

Since the relation of e_f as a function of w_{max} is the same as in the monotonic law, the differentiation of Eq. (4) when applied to the fatigue damage parameter e_f provides

$$\frac{de_f}{dw_{max}} = \frac{w_u w_o}{w_{max}^2(w_u - w_o)} \tag{9}$$

The second term of Eq. (8) defines the evolution of w_{max} as a function of the local damaged area $A_{p(k)}$. Assuming that the ratio between $A_{p(k)}$ and the area corresponding to each integration point $A_{t(k)}$ is the same as the ratio between the dissipated energy G_{Id} (Fig. 1) and the fracture energy G_{Ic} (Turon et al., 2007), it gives

$$\frac{A_{p(k)}}{A_{t(k)}} = \frac{G_{Id}}{G_{Ic}} \tag{10}$$

In a two-dimensional finite element analysis $A_{t(k)} = Bl_p$ being B the constant width and l_p the length corresponding to IP k, which depends on the element size and on the weight of the IP in the integration method considered. From Fig. 1, the dissipated energy can be written as

$$G_{Id} = G_{Ic} - \frac{\sigma_{(w_{max})} w_u}{2} \tag{11}$$

being

$$\sigma_{(w_{max})} = (1 - e)\frac{\sigma_u}{w_o} w_{max} \tag{12}$$

Combining Eqs. (1), (4), (11) and (12), Eq. (10) leads to

$$w_{max} = \frac{A_{p(k)}(w_u - w_o)}{A_{t(k)}} + w_o \tag{13}$$

and

$$\frac{dw_{max}}{dA_{p(k)}} = \frac{w_u - w_o}{A_{t(k)}} \tag{14}$$

Substituting Eqs. (14) and (9) in Eq. (8) it gives

$$\frac{de_f}{dA_{p(k)}} = \frac{w_u w_o}{w_{max}^2 A_{t(k)}} \tag{15}$$

The second term of Eq. (7) represents the growth rate of the damaged area associated with each IP as a function of the number of cycles. Assuming that there are several IPs in the FPZ (that number is assumed to be n_{FPZ}) undergoing fatigue loading, the global fatigue crack growth rate can be given by the weighted average (accounting for the relative weight of each IP in the integration scheme used) of the local damaged area growth of all n_{FPZ} points, i.e.,

$$\frac{dA}{dN} = \sum_{k=1}^{n_{FPZ}} \frac{dA_{p(k)}}{dN} \tag{16}$$

being $dA = Bda$, where da is the increment of crack length. The global fatigue crack growth rate can also be given by the modified Paris law (Pirondi and Moroni, 2010), which relates it to the range of the strain energy release rate applied cyclically ΔG_I,

$$\frac{dA}{dN} = C_1 \left(\frac{\Delta G_I}{G_{Ic}}\right)^{C_2} \tag{17}$$

where C_1 and C_2 are empirical material parameters derived from experimental data. Assuming that the same fatigue law is valid

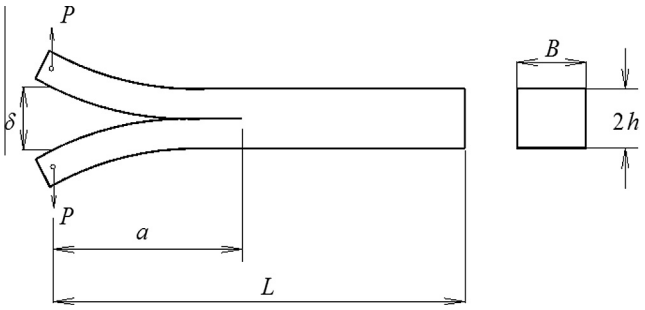

Fig. 3. Schematic representation of the DCB test.

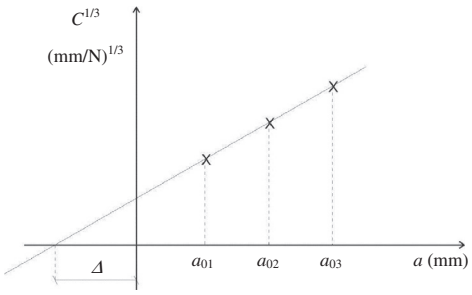

Fig. 5. Schematic representation of the crack length correction Δ determination.

Table 1
Typical elastic properties of carbon-epoxy.

E_1 = 150 GPa	ν_{12} = 0.34	G_{12} = 4315 MPa
E_2 = 8819 MPa	ν_{13} = 0.34	G_{13} = 4315 MPa
E_3 = 8819 MPa	ν_{23} = 0.38	G_{23} = 3200 MPa

for each IP k, the contribution of each IP in the FPZ to global damage growth can be given by

$$\frac{dA_{p(k)}}{dN} = \frac{C_1 r_w}{n_{FPZ}} \left(\frac{\Delta G_{Ik}}{G_{Ic}}\right)^{C_2} \tag{18}$$

where r_w represents the relative weight of each integration point. In the present case the Newton–Cotes integration scheme was used, which is based on the Simpson's 1/3 rule considering the three IPs of each cohesive element, whose relative weights are (1,4,1), respectively (Balagurusamy, 1999). The modified Paris law can be expressed as (Eqs. (16) and (18))

$$\frac{dA}{dN} = \sum_{k=1}^{n_{FPZ}} \frac{C_1 r_w}{n_{FPZ}} \left(\frac{\Delta G_{Ik}}{G_{Ic}}\right)^{C_2} \tag{19}$$

In high cycle fatigue the material behaves essentially in the elastic regime. Defining the load ratio in a cycle as $R = P_{min}/P_{max}$ and considering that $G_I = f(P^2)$ (see Eq. (26) in the next section) it can be written

$$\Delta G_{Ik} = (1 - R^2) G_{Ik_{max}} \quad \text{with} \quad R^2 = \frac{G_{Ik_{min}}}{G_{Ik_{max}}} \tag{20}$$

where $G_{Ik_{min}}$ and $G_{Ik_{max}}$ are the values of G_I for IP k, for the applied load P_{min} and P_{max}, respectively. From Eq. (20) it can be observed that, for a given load ratio R, the range of the strain energy release rate applied cyclically ΔG_{Ik} only depends on $G_{Ik_{max}}$. The accurate determination of the $G_{Ik_{max}}$ values in each IP k is an important aspect of the method. The following relation (Rice, 1968)

$$G_{Ik_{max}} = \int_0^w \sigma \, dw \tag{21}$$

can be written in a discrete form as (Kawashita and Hallett, 2012)

$$G_{Ik_{max}} = \sum_{i=1}^{n_{inc}} \left(\frac{\sigma_i + \sigma_{i-1}}{2}\right)(w_i - w_{i-1}) \tag{22}$$

where n_{inc} represents the current increment number. Following this relation, the actual value of $G_{Ik_{max}}$ is calculated via a successive sum of energy increments. In a given increment i of the loading history the increase of $G_{Ik_{max}}$ is obtained from the product of the average traction by the variation of relative displacement. Since σ_i is a function of e_f, which in turn depends on $G_{Ik_{max}}$, an iterative procedure involving these parameters is necessary. The iterative process stops when the difference of σ_i between two consecutive iterations becomes less than a pre-established small residual.

Substituting Eqs. (15) and (18) into Eq. (7) the variation of the fatigue damage parameter (Δe_f) for a given increase in the number of cycles ΔN at a given IP k belonging to the FPZ becomes

$$\Delta e_f(\Delta N) = \frac{w_u w_o C_1 r_w}{w_{max}^2 B l_p n_{FPZ}} \left(\frac{\Delta G_{Ik}}{G_{Ic}}\right)^{C_2} \Delta N \tag{23}$$

The definition of ΔN is dictated by a pre-defined maximum variation allowed for the damage parameter of the IPs belonging to the FPZ. The choice of Δe_{max} is a compromise between CPU time and accuracy of the results.

2.3. Numerical analysis

In order to validate the proposed method, a numerical analysis of a DCB test considering a carbon-epoxy composite bonded joint was performed. The dimensions of the DCB specimen were $2h$ = 5.4 mm, B = 25 mm, a_0 = 45 mm and the specimen's total length 125 mm (Fig. 3). A two-dimensional analysis using 744 8-node plane stress elements and 160 6-node cohesive elements connecting the plane elements at the mid-thickness of the specimen was performed. Typical elastic properties of unidirectional carbon-epoxy laminates are listed in Table 1. From a previous work (de Moura et al., 2008) the critical strain energy release rate and cohesive strength were assumed to be G_{Ic} = 0.43 N/mm and σ_u = 30 MPa. The modified Paris law parameters were initially considered to be C_1 = 16.0 mm^2/cycle and C_2 = 6.0. These values lead to complete failure around 70,000 cycles which was considered reasonable for the first analysis. A loading envelope similar to the one presented in Fig. 2 was employed. An initial quasi-static loading up to 75 N was applied followed by high-cycle fatigue with R^2 = 0, i.e., a sinusoidal cyclic load oscillating between zero and a maximum constant value (75 N). A more refined mesh (element length equal to 0.125 mm – Fig. 4) was generated in the region corresponding to damage propagation to guarantee stable crack growth. The jump cycle was dictated by the maximum variation allowed for the damage parameter Δe_{max}. A value of Δe_{max} = 0.1% was verified to provide convergent solutions in a reasonable analysis duration.

Fig. 4. The mesh used – diagonal crosses identify the cohesive elements.

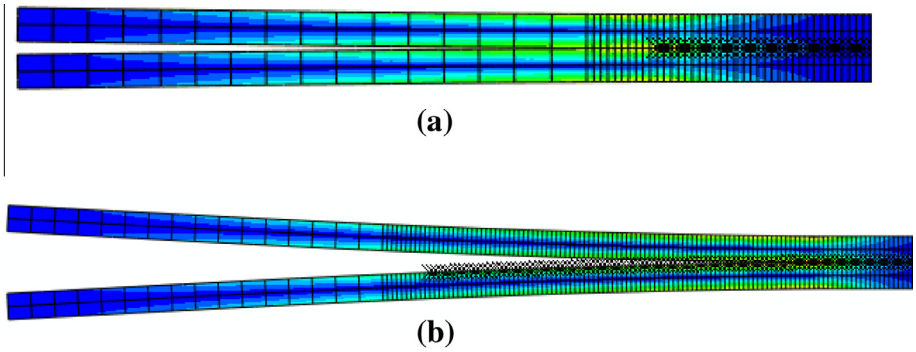

Fig. 6. Deformed shape (a) detail at the beginning of the fatigue loading step and (b) at its end.

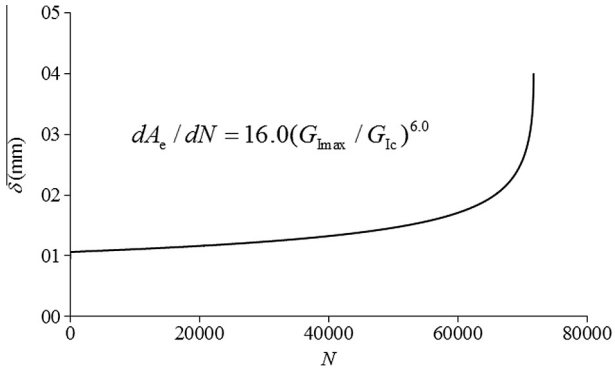

Fig. 7. Evolution of applied displacement (δ) as a function of the number of cycles (N) using the given modified Paris law.

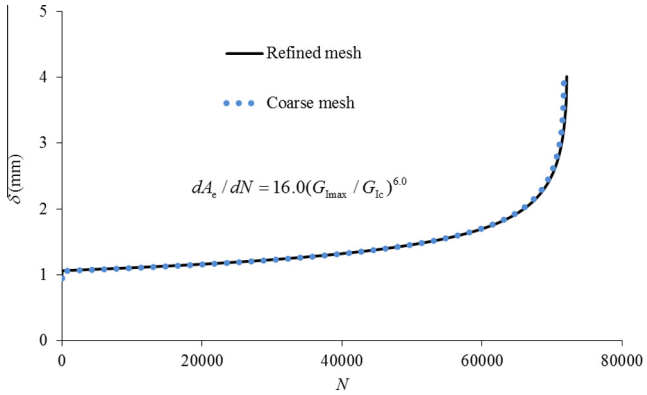

Fig. 10. Displacement versus number of cycles curves considering two different meshes.

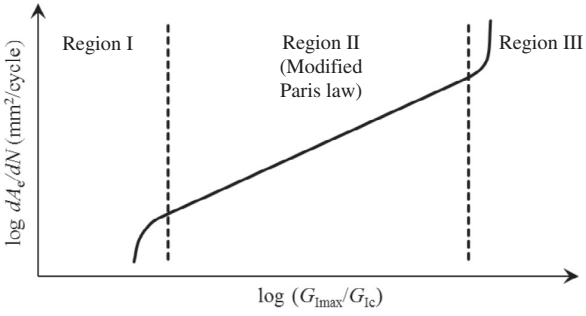

Fig. 8. Typical fatigue crack growth rate versus the ratio of strain energy release rate in a bi-logarithm scale.

2.4. Data reduction scheme

An equivalent crack method previously developed for quasi-static problems (de Moura et al., 2008) was applied to obtain the evolution of the strain energy release rate. In fact, it is not easy to monitor the crack length with the required accuracy during experimental fatigue tests. The proposed method overcomes this difficulty since it employs the specimen's compliance ($C = \delta/P$) to estimate an equivalent crack length. From the Timoshenko beam theory,

$$C = \frac{8a^3}{E_1 B h^3} + \frac{12a}{5BhG_{13}} \tag{24}$$

where E_1, G_{13} are the longitudinal and shear modulus, respectively and a is the current crack length. An equivalent flexural modulus E_f can be obtained from the previous equation using the initial

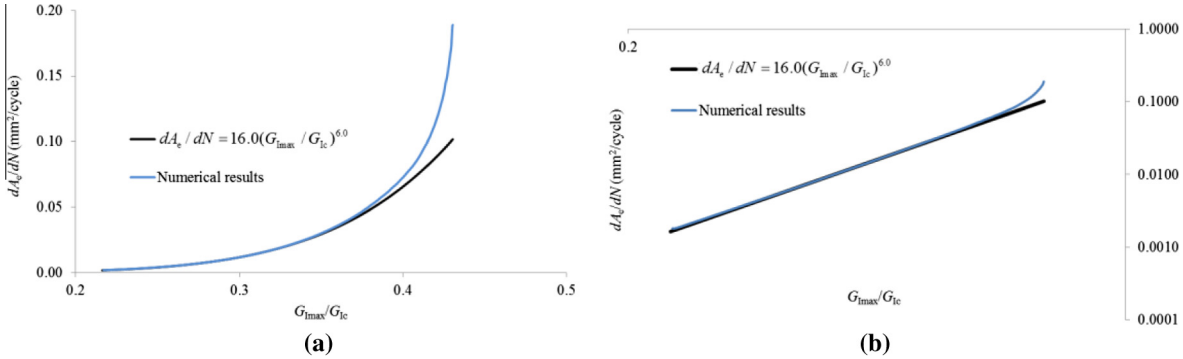

Fig. 9. Crack growth rate (dA_e/dN) as a function of strain energy release rate ratio (G_{Imax}/G_{Ic}) in (a) normal and (b) bi-logarithmic scales.

conditions (a_0 and C_0). This procedure accounts for several aspects not included in the beam theory, as is the case of the adhesive presence, stress concentrations and material variability between different specimens. The expression for E_f is given by

$$E_f = \left(C_0 - \frac{12(a_0+\Delta)}{5BhG_{13}}\right)^{-1} \frac{8(a_0+\Delta)^3}{Bh^3} \tag{25}$$

where root rotation effects are included through the crack length correction Δ. A simple numerical procedure can be used to determine Δ. In fact, the elastic modulus of the specimen can be assessed by fitting the initial stiffness of the numerical load–displacement curve with the experimental one. Afterwards, two additional numerical simulations considering different initial crack lengths are performed in order to obtain three points in the $C^{1/3} = f(a)$ plot (Fig. 5). The intersection of this relation with the horizontal axis defines the value of Δ.

The evaluation of G_I in the course of the fatigue test employing data reduction schemes based on crack length monitoring is a difficult task, namely in the case of ductile adhesives that develop

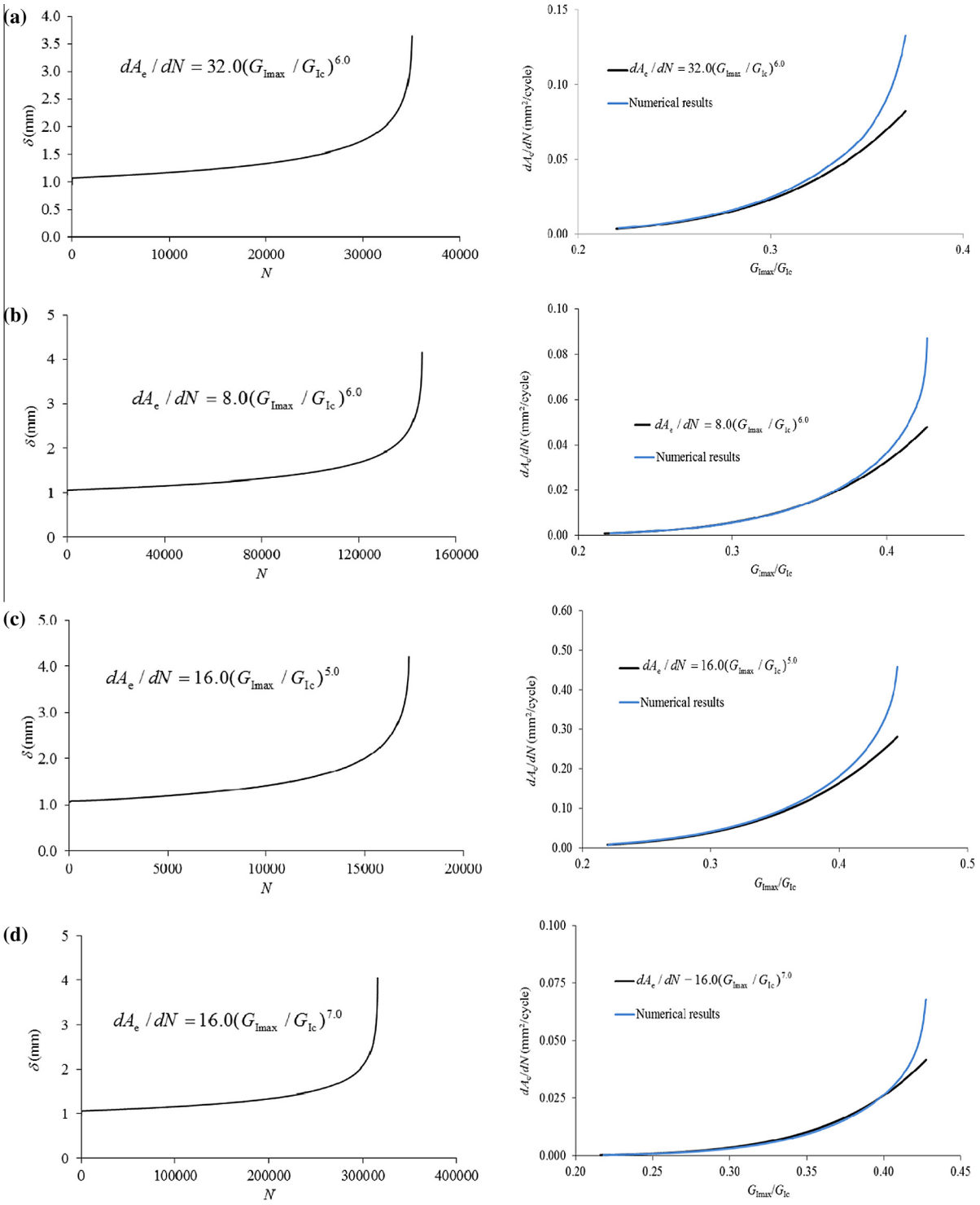

Fig. 11. Displacement evolution and crack growth rate considering different values of the Paris law parameters: (a) C_1 = 32.0 mm²/cycle; (b) C_1 = 8.0 mm²/cycle; (c) C_2 = 5.0; (d) C_2 = 7.

pronounced FPZ. To overcome this drawback, Eq. (24) can be used to calculate an equivalent crack length from the current compliance. The Matlab® software can be used to solve the cubic equation $a_e = f(C)$. Finally, the evolution of the strain energy release rate as a function of the equivalent crack length can be obtained combining the Irwin–Kies equation

$$G_I = \frac{P^2}{2B}\frac{dC}{da} \tag{26}$$

with Eq. (24), giving rise to

$$G_I = \frac{6P^2}{B^2 h}\left(\frac{2a_e^2}{E_f h^2} + \frac{1}{5G_{13}}\right) \tag{27}$$

Following this procedure the crack length does not need to be monitored during the fatigue test, since the equivalent crack and the strain energy release rate are obtained using exclusively data resulting from the evolution of displacement (assuming that a constant loading amplitude (Fig. 2) is applied). Furthermore, the energy dissipated in a non-negligible fracture process zone, typical of ductile adhesives, is indirectly taken into account by means of the current specimen's compliance used.

3. Results

Since a load control test with constant amplitude loading was considered in the analysis, the material fatigue degradation induces an increase of applied displacement during the test. Fig. 6 presents the deformed shape at the beginning of the fatigue loading process and at its end. It is clearly visible that significant propagation has occurred. In Fig. 7 it can be observed that a gradual increase of applied displacement takes place till 60,000 cycles, after which a remarkable augment is evident leading to catastrophic failure at approximately 70,000 cycles. This high rate displacement is due to the increase of fatigue crack growth (FCG) rate induced by the rise of strain energy release rate (G_{Imax}) that becomes close to the critical value (G_{Ic}). This corresponds to the so-called third region of fatigue crack growth rate (Fig. 8) characterised by unstable and catastrophic crack propagation leading to the specimen's final failure. This behaviour is outside the scope of the Paris law, which only applies to the second region of FCG rate described by a linear correlation (Fig. 8) of the relation $dA_e/dN = f(G_{Imax}/G_{Ic})$ in a bi-logarithm scale. It can then be concluded that the model is able to manage well the effects of damage accumulation during sub-critical cyclic loading.

Considering exclusively the $\delta = f(N)$ curve (Fig. 7) and applying the equivalent crack length procedure, the relationship between FCG rate (dA_e/dN) and the strain energy release rate ratio (G_{max}/G_{Ic}) can be obtained. Fig. 9 compares the input and resultant relations in normal and bi-logarithmic scale. It can be observed that excellent agreement exists from the beginning of the fatigue test simulation till a certain point, becoming gradually divergent in the final part of the test. This behaviour is in agreement with the fact that the Paris law is only valid in the second region of FCG rate. However, as already discussed, the proposed model is able to identify the third region of FCG rate where deviation between the input law and numerical results becomes evident.

In order to perform a mesh sensitivity analysis two different meshes with 0.125 mm and with 0.0625 mm elements length in the region of crack propagation were used. One crucial aspect is the number of IPs in the FPZ (n_{FPZ}), which is approximately double in the refined mesh relative to the other one, during the course of the test simulation. The corresponding displacement versus number of cycles curves are plotted in Fig. 10. A close agreement was obtained which demonstrates that the proposed model is not mesh dependent, which means that the results are insensitive to n_{FPZ}.

The aptitude of the proposed fatigue cohesive model to deal with different Paris laws was also examined. In this context, numerical simulations considering different values of C_1 and C_2 parameters were performed. Fig. 11(a) and (b) depict the alteration of parameter C_1 by multiplying and dividing, respectively, its original value ($C_1 = 16\ mm^2/cycle$) by a factor of 2. The increase of C_1 (Fig. 11(a)) induces an increase of crack growth rate which means that final failure occurs earlier (approximately 45,000 cycles

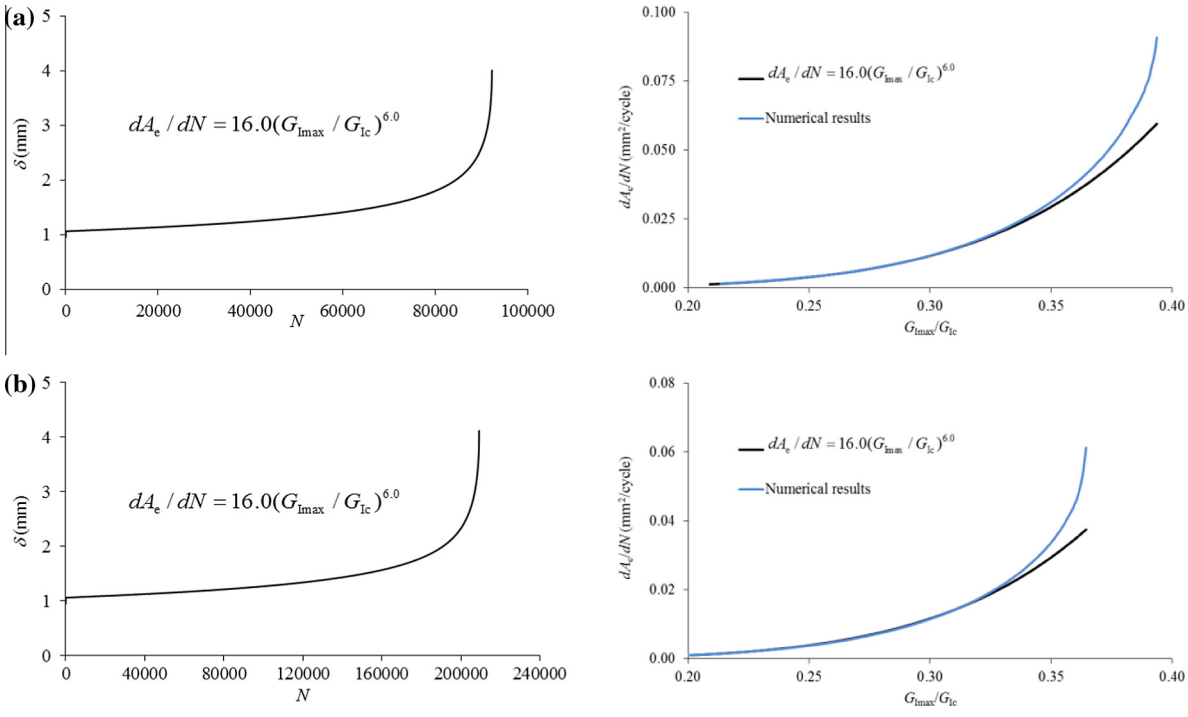

Fig. 12. Displacement evolution and crack growth rate considering different values of load ratio: (a) $R = 0.2$; (b) $R = 0.4$.

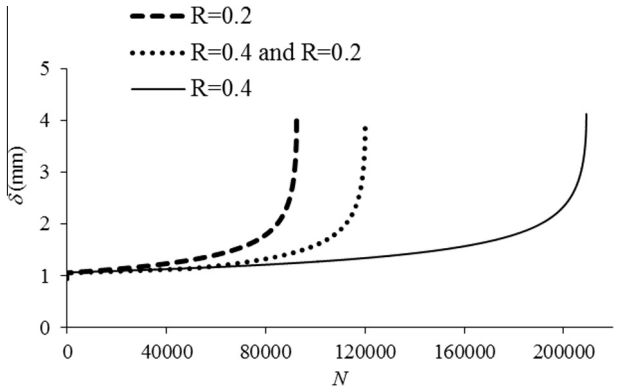

Fig. 13. Comparison of displacement evolution considering different load ratios *R*.

instead of the previous 70,000 (Fig. 7), thus leading to premature deviation between the input and numerical $dA_e/dN = f(G_{Imax}/G_{Ic})$ curves. The opposite trend can be observed in Fig. 11(b) owing to the reduction of C_1. The influence of C_2 was assessed by varying it by unity from the reference value ($C_2 = 6$). The decrease of C_2 leads to a rise on the dA_e/dN (Fig. 11(c)) since the ratio G_{Imax}/G_{Ic} is always smaller than one during fatigue crack growth. It can be observed that this parameter has a remarkable influence since the drastic propagation occurred below 20,000 cycles. Accordingly, the agreement between the input and numerical $dA_e/dN = f(G_{Imax}/G_{Ic})$ curves is confined to their beginning. Once again, the opposite tendency is observed when $C_2 = 7$; in this case abrupt failure happens for 300,000 cycles and the range of the Paris law occurs for a large extent of $dA_e/dN = f(G_{Imax}/G_{Ic})$ curves. Finally, it should be emphasised that the numerical model was able to reproduce with accuracy the crack growth rate in all the cases in the region of applicability of the modified Paris law.

Another aspect that was analysed was the effect of load ratio $R = P_{min}/P_{max}$. Fig. 12(a) and (b) report to simulations of the DCB test considering load ratios equal to 0.2 and 0.4, respectively. As expected, the increase of *R*, which corresponds to smaller loading amplitude, causes longer fatigue life, i.e. drastic failure changes from 90,000 to more than 200,000 cycles. The comparison between the input and resultant FCG curves reveals that the model is able to accurately capture all the described effects in the region where the modified Paris law is applicable.

Fig. 13 compares the evolution of the displacement of a case with load ratio variation – $R = 0.4$ up to 50,000 cycles followed by a loading cycling with $R = 0.2$ till final failure – with previous cases with constant load ratio ($R = 0.4$ and $R = 0.2$) during the entire fatigue test. As expected an in-between behaviour can be observed. The $\delta = f(N)$ curve of the load ratio variation case starts to diverge from the $R = 0.4$ curve at 50,000 cycles leading to fatigue failure much earlier. On the other hand, when compared with the $R = 0.2$ loading case, the final failure occurs later owing to the less severe fatigue loading ($R = 0.4$) in the earliest 50,000 cycles. It can be settled that the model reproduces well this logical and expected behaviour.

4. Conclusions

A cohesive zone model for mode I high cycle fatigue simulation of adhesively bonded joints is presented in this work. The method is based on the Paris law and performs stiffness degradation as a function of number of cycles by means of a damage parameter that includes static and fatigue softening. The model was validated numerically using the finite element method in the simulation of the double cantilever beam test. In the validation procedure, different modified Paris laws and loading conditions were used as input in the numerical model. Subsequently, the numerical results were treated to verify the agreement of the fatigue crack growth curves with those used as input. A mesh sensitivity analysis proved that the model does not depend on mesh refinement. A previously developed equivalent crack length based method for monotonic analysis applied to the double cantilever beam test was also used in the context of the simulation of fatigue tests.

Different modified Paris law parameters were employed and it was verified that the numerical results show excellent agreement with the input laws, in the region corresponding to the applicability of the modified Paris law. This is a crucial issue since it demonstrates that the model is able to accurately simulate the fatigue crack growth rate as a function of the number of cycles under different circumstances.

In addition, the model was tested for cases with different load ratios as well as in a case of load ratio variation during the fatigue test. The load ratio plays an important role in the fatigue life since it is a measure of amplitude loading. In all cases the model demonstrated its ability to deal with all of these situations.

In summary, it can be concluded that the two major aspects influencing fatigue behaviour, which are the load magnitude and its amplitude are very well captured by the proposed model.

References

Balagurusamy, E., 1999 (Numerical Methods). Tata McGraw-Hill, ISBN 978-0-07-463311-3.
Barenblatt, G.I., 1962. The mathematical theory of equilibrium cracks in brittle fracture. Adv. Appl. Mech. 7, 55–129.
de Moura, M.F.S.F., Campilho, R.D.S.G., Gonçalves, J.P.M., 2008. Crack equivalent concept applied to the fracture characterization of bonded joints under pure mode I loading. Compos. Sci. Technol. 68, 2224–2230.
de Moura, M.F.S.F., Gonçalves, J.P.M., Magalhães, A.G., 2012. A straightforward method to obtain the cohesive laws of bonded joints under mode I loading. Int. J. Adhes. Adhes. 39, 54–59.
de Moura, M.F.S.F., Gonçalves, J.P.M., Marques, A.T., de Castro, P.M.S.T., 2000. Prediction of compressive strength of carbon-epoxy laminates containing delamination by using a mixed-mode damage model. Compos. Struct. 50, 151–157.
Dugdale, D.S., 1960 (Yielding of steel sheets containing slits). J. Mech. Phys. Solids 8, 100–104.
Gonçalves, J.P.M., de Moura, M.F.S.F., de Castro, P.M.S.T., Marques, A.T., 2000. Interface element including point-to-surface constraints for three-dimensional problems with damage propagation. Eng. Comput.: Int. J. Comput. Aided Eng. Softw. 17, 28–47.
Gonçalves, J.P.M., de Moura, M.F.S.F., Magalhães, A.G., de Castro, P.M.S.T., 2003. Application of interface finite elements to three-dimensional progressive failure analysis of adhesive joints. Fatigue Fract. Eng. Mater. Struct. 26, 479–486.
Harper, P.W., Hallett, S.R., 2010. A fatigue degradation law for cohesive interface elements – development and application to composite materials. Int. J. Fatigue 32, 1774–1787.
Hillerborg, A., Modeer, M., Petersson, P.E., 1976. Analysis of crack formation and crack growth in concrete by means of fracture mechanics and finite elements. Cem. Concr. Res. 6, 773–781.
Katnam, K.B., Crocombe, A.D., Khoramishad, H., Ashcroft, I.A., 2010. Load ratio effect on the fatigue behaviour of adhesively bonded joints: an enhanced damage model. J. Adhes. 86, 257–272.
Kawashita, L.F., Hallett, S.R., 2012. A crack tip tracking algorithm for cohesive interface element analysis of fatigue delamination propagation in composite materials. Int. J. Solids Struct. 49, 2898–2913.
Khoramishad, H., Crocombe, A.D., Katnam, K.B., Ashcroft, I.A., 2010a. A generalised damage model for constant amplitude fatigue loading of adhesively bonded joints. Int. J. Adhes. Adhes. 30, 513–521.
Khoramishad, H., Crocombe, A.D., Katnam, K.B., Ashcroft, I.A., 2010b. Predicting fatigue damage in adhesively bonded joints using a cohesive zone model. Int. J. Fatigue 32, 1146–1158.
May, M., Hallett, S.R., 2010. A combined model for initiation and propagation of damage under fatigue loading for cohesive interface elements. Compos. Part A 41, 1787–1796.
Mi, U., Crisfield, M., Davies, G., 1999. Progressive delamination using interface elements. J. Compos. Mater. 32, 1246–1272.
Moroni, F., Pirondi, A., 2011. A procedure for the simulation of fatigue crack growth in adhesively bonded joints based on the cohesive zone model and different mixed-mode propagation criteria. Eng. Fract. Mech. 78, 1808–1816.
Muñoz, J.J., Galvanetto, U., Robinson, P., 2006. On the numerical simulation of fatigue driven delamination using interface elements. Int. J. Fatigue 28, 1136–1146.

Nguyen, O., Repetto, E.A., Ortiz, M., Radovitzky, R.A., 2001. A cohesive model of fatigue crack growth. Int. J. Fract. 110, 351–369.
Pirondi, A., Moroni, F., 2010. A progressive damage model for the prediction of fatigue crack growth in bonded joints. J. Adhes. 86, 501–521.
Reddy Jr., E.D., Mello, F.J., Guess, T.R., 1997. Modeling the initiation and growth of delaminations in composite structures. J. Compos. Mater. 31, 940–977.
Rice, J.R., 1968. A path independent method integral and the approximate analysis of strain correlation by notches and cracks. ASME J. Appl. Mech. 35, 379–386.
Robinson, P., Galvanetto, U., Tumino, D., Bellucci, G., Violeau, D., 2005. Numerical simulation of fatigue-driven delamination using interface elements. Int. J. Numer. Methods Eng. 63, 1824–1848.
Roe, K.L., Siegmund, T., 2003. An irreversible cohesive zone model for interface fatigue crack growth simulation. Eng. Fract. Mech. 70, 209–232.
Schellekens, J., de Borst, R., 1993. A nonlinear finite-element approach for the analysis of mode-I free edge delamination in composites. Int. J. Solids Struct. 30, 1239–1253.
Sørensen, B.F., 2002. Cohesive law and notch sensitivity of adhesive joints. Acta Mater. 50, 1053–1061.
Turon, A., Costa, J., Camanho, P.P., Dávila, C.G., 2007. Simulation of delamination in composites under high-cycle fatigue. Compos. Part A 38, 2270–2282.
Wahab, M.M.A., 2012. Fatigue in adhesively bonded joints: a review. ISRN Mater. Sci. 2012, 25p (Article ID 746308). http://dx.doi.org/10.5402/2012/746308.
Yang, Q.D., Thouless, M.D., Ward, S.M., 1999. Numerical simulations of adhesively-bonded beams failing with extensive plastic deformation. J. Mech. Phys. Solids 47, 1337–1353.